

# Demonstration of Broadband Wavelength Conversion at 40 Gb/s in Silicon Waveguides

Benjamin G. Lee, *Student Member, IEEE*, Aleksandr Biberman, *Student Member, IEEE*, Amy C. Turner-Foster, Mark A. Foster, Michal Lipson, *Senior Member, IEEE*, Alexander L. Gaeta, and Keren Bergman, *Fellow, IEEE*

**Abstract**—We present ultra-broadband wavelength conversion in silicon photonic waveguides at a data rate of 40 Gb/s. The dispersion-engineered device demonstrates a conversion bandwidth spanning the entire *S*-, *C*-, and *L*-bands of the ITU grid. Using a continuous-wave *C*-band pump, an input signal of wavelength 1513.7 nm is up-converted across nearly 50 nm at a data rate of 40 Gb/s, and bit-error-rate measurements are performed on the converted signal.

**Index Terms**—Optical frequency conversion, optical Kerr effect, optical signal processing, silicon-on-insulator technology.

## I. INTRODUCTION

THE silicon material system is continually being utilized to demonstrate optical devices that deliver exceptional performance, and researchers are exploiting the benefits of these devices for diverse applications, ranging from short-haul optical communications links [1] to on-chip global interconnection networks [2]. The most notable appeal of silicon photonics stems from its complementary metal–oxide–semiconductor process compatibility, which allows low-cost, high-yield fabrication of monolithically integrated circuits that can combine optical and electrical functionalities. The large index contrast enables waveguides with low bending losses and engineered dispersions, empowering a broad and flexible photonic circuit design space complemented with immense dispersion tunability [3]. Leveraging this wide dispersion tuning capability, silicon waveguides have recently become a promising platform for ultrafast all-optical parametric processing. As a result, silicon wavelength converters [4]–[7], amplifiers [8], and regenerators [9] based on four-wave mixing (FWM) have been demonstrated. These processing capabilities represent essential functionalities to future transparent optical networks, where it is envisioned that low-level processing will be performed in the optical domain when possible in order to allow wavelength

channels with data rates approaching 1 Tb/s to transparently route through complex network architectures. For instance, current access networks may benefit from such processing capabilities by providing data aggregation at edge nodes via ultrafast all-optical manipulation of high-speed data streams, alleviating bottlenecks at current optical–electrical–optical conversions [10].

Previously, FWM-based wavelength conversion in silicon waveguides has been demonstrated with greater than 150-nm bandwidths using continuous-wave (CW) pumping [5]. Moreover, conversion efficiencies have been repeatedly demonstrated in the vicinity of  $-10$  dB for both 10-Gb/s [4]–[6] and 40-Gb/s [7] signals. In these studies, the analysis of the converted optical data streams has been most frequently performed using qualitative time-domain (eye diagrams) and frequency-domain (output spectra) tactics available at the physical layer. However, quantitative data performance metrics, such as bit-error rate (BER) and power penalty, had not been shown until recently. In [11], we were among the first to report quantitative systems-level measurements on FWM-based silicon wavelength converters, demonstrating error-free (BER less than  $10^{-12}$ ) 35-nm wavelength conversion at a data rate of 10 Gb/s, and error-free 12-nm conversion at 40 Gb/s. As we reported these results, Mathlouthi *et al.* [12] also reported a systems-level characterization of silicon wavelength converters (in comparison to semiconductor optical amplifier-based converters) demonstrating two-channel conversion at 40-Gb/s across 2.5 and 4 nm for the two channels. In this letter, we report on significant improvements to our former results, extending the 40-Gb/s testbed-limited conversion bandwidth to 47.7 nm, the largest high-speed conversion reported to date, using a device with bandwidth covering the entire ITU *S*-, *C*-, and *L*-bands. Furthermore, we measure a minimum power penalty of 2.9 dB on the converted signal at a BER of  $10^{-9}$ .

## II. DEVICE AND EXPERIMENTS

The device is a 1.1-cm-long waveguide fabricated at the Cornell Nanofabrication Facility using electron-beam lithography followed by reactive-ion etching. The waveguide thickness is measured to be 290 nm with a slab thickness of 25 nm. The waveguide width is 680 nm. Each end of the waveguide has an inverse taper for efficient coupling to tapered fibers. Fiber-to-fiber losses (including coupling loss and propagation loss) were less than 8 dB for the device.

The setup for BER measurements (Fig. 1) consists of a CW pump beam coupled to a nonreturn-to-zero (NRZ) modulated probe beam through a dense wavelength-division multiplexer (DWDM). The probe is modulated with a pseudorandom bit sequence (PRBS) of length  $2^{15} - 1$  generated by a 40-Gb/s pattern

Manuscript received August 18, 2008; revised November 07, 2008. First published December 09, 2008; current version published January 16, 2009.

This work was supported in part by the DARPA MTO Parametric Optical Processes and Systems Program under Contract W911NF-08-1-0058.

B. G. Lee, A. Biberman, and K. Bergman are with the Department of Electrical Engineering, Columbia University, New York, NY 10027 USA (e-mail: benlee@ee.columbia.edu; biberman@ee.columbia.edu; bergman@ee.columbia.edu).

A. C. Turner-Foster, M. Lipson are with the School of Electrical and Computer Engineering, Cornell University, Ithaca, NY 14853 USA (e-mail: act28@cornell.edu; lipson@ece.cornell.edu).

M. A. Foster, A. L. Gaeta are with the School of Applied and Engineering Physics, Cornell University, Ithaca, NY 14853 USA (e-mail: maf42@cornell.edu; a.gaeta@cornell.edu).

Color versions of one or more of the figures in this letter are available online at <http://ieeexplore.ieee.org>.

Digital Object Identifier 10.1109/LPT.2008.2009945

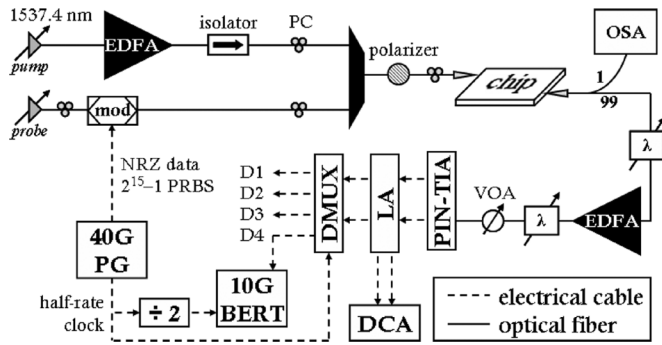


Fig. 1. Experimental setup. (BERT: bit-error-rate tester; DCA: digital communications analyzer; DMUX: 1:4 demultiplexer;  $\lambda$ : tunable grating filter; LA: limiting amplifier with 1:2 fanout; mod: LiNbO<sub>3</sub> modulator; PC: polarization controller; PIN-TIA: optical receiver with p-i-n photodiode and transimpedance amplifier; 40G PG: 40-Gb/s pattern generator; VOA: variable optical attenuator.)

generator (PG). The lightwaves then pass through a fiber-optic polarizer and a polarization controller (PC) facilitating insertion into the waveguide along the transverse-electric polarization. Before injection, the pump and average probe powers are 22.8 and 6.2 dBm, respectively. The output power is monitored on an optical spectrum analyzer (OSA), while the converted signal is separated from the pump and probe by a tunable grating filter with a 3-dB passband of 1.3 nm. An erbium-doped fiber amplifier (EDFA) is used for preamplification, and a second filter is used to block extraneous amplified spontaneous emissions (ASE). A p-i-n photodiode and transimpedance amplifier (PIN-TIA), along with a limiting amplifier, receive the optical signal. Next, the 40-Gb/s differential data signal is demultiplexed to four single-ended 10-Gb/s streams, and each is independently analyzed using a digital communications analyzer and a BER tester. The 10-GHz clock signal used for error analysis is obtained from the 20-GHz half-rate clock output of the PG following a divide-by-two circuit. The half-rate clock also drives the demultiplexer.

The conversion efficiency of the silicon waveguide is plotted versus injected pump power (Fig. 2), measured just before insertion into the input tapered fiber. A near-quadratic relationship is observed as expected from theory [13]. At high pump powers (greater than 24 dBm), the gains in conversion efficiency begin to roll-off due to excessive loss caused by two-photon absorption (TPA)-induced free-carrier absorption. In the same figure, the wavelength dependence of the device is characterized. Only the long-wavelength side of the curve is fully explored because our tunable lasers operate only at wavelengths longer than 1510 nm; however, reasonable symmetry is expected. The 3-dB conversion bandwidth, defined as the difference between the input probe wavelength and the converted signal wavelength, exceeds 110 nm for the measured device. The drop in efficiency outside of this range is attributed to the dispersion-induced phase mismatch.

Despite the enormous conversion bandwidth of the silicon waveguide, practical high-speed data measurements are limited by the wavelength dependence of the required commercial components. First, following the conversion, preamplification is required to reach the 100- $\mu$ W sensitivity level of the 40-Gb/s PIN-TIA receiver. Therefore, the output signal is targeted in the C-band where gain from an EDFA is available. Second,

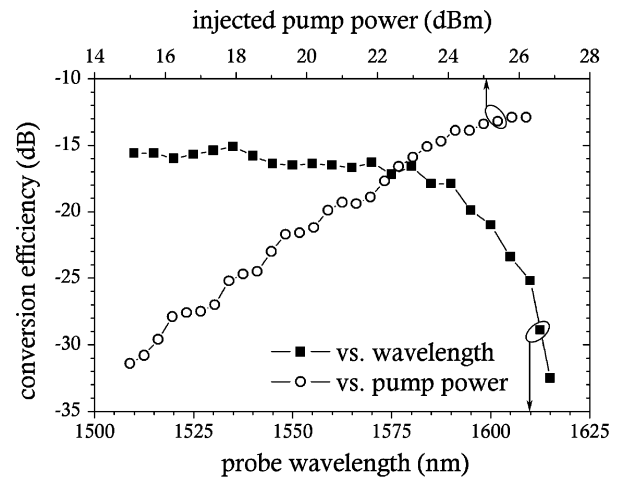


Fig. 2. Bottom axis: conversion efficiency versus input probe wavelength with a pump wavelength of 1537 nm and a pump injection power of 24 dBm. Top axis: conversion efficiency as a function of injected pump power with the same pump wavelength and a probe wavelength of 1514 nm.

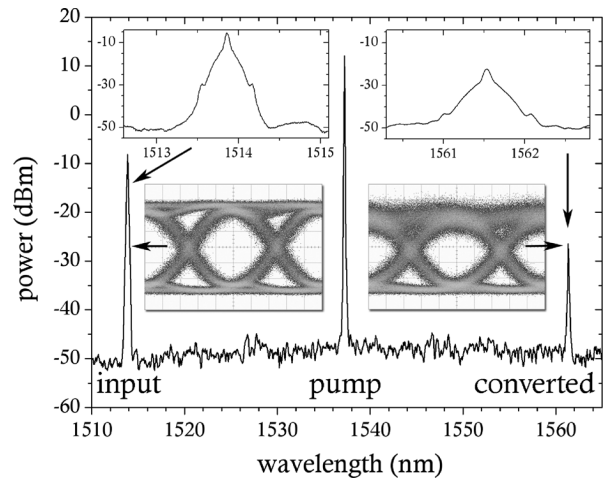


Fig. 3. Spectrum showing 47.7-nm conversion of a 40-Gb/s data signal. The amplitude reflects the fiber-coupled power following the chip. Insets show close-up spectra (OSA resolution bandwidth of 0.06 nm) and eye diagrams (time span of 50 ps). The input eye is taken before injection into the chip.

the tunable bandpass filters used for demultiplexing and ASE filtering are specified to operate at wavelengths shorter than 1560 nm, further restricting the possible conversion window. (We were able to use them at wavelengths up to 1561.5 nm.) Finally, as mentioned previously, our tunable laser sources were constrained to a minimum wavelength of 1510 nm.

### III. RESULTS

We selected a DWDM operating on channel C50 of the ITU C-band to couple the pump and probe beams. The pump and probe wavelengths were chosen in order to provide the largest conversion bandwidth allowable by the tunable filters and tunable laser. A sample OSA trace (Fig. 3) depicts the 47.7-nm conversion, from an input probe wavelength of 1513.7 nm to a converted wavelength of 1561.4 nm with conversion efficiency near  $-18$  dB at a data rate of 40 Gb/s. The conversion losses cause a noticeable degradation in optical signal-to-noise ratio (OSNR) of the converted signal [Fig. 3 (inset)]. For this reason,

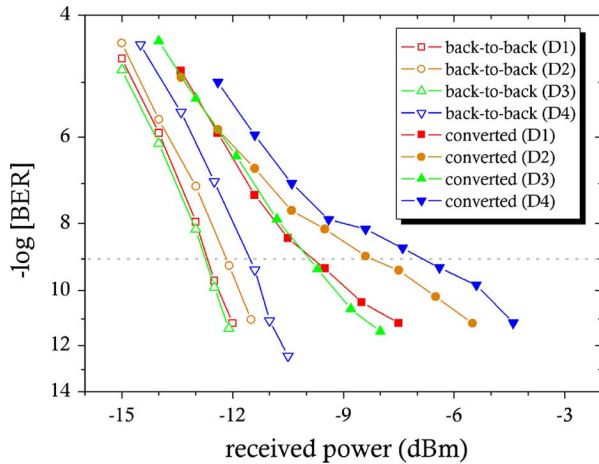


Fig. 4. The 40-Gb/s BER curves taken on each of the demultiplexer outputs D1–D4 after wavelength conversion (filled symbols) with their back-to-back cases taken directly after modulation (open symbols).

the efficiency of the wavelength converter is one of its most crucial parameters for systems-level integration. Converters with efficiencies of  $-8.5$  dB have been reported using CW pumping [6] and of 5.2 dB using pulsed pumps [8]. Further advances are expected in CW devices that create an electric field in the waveguide's transverse direction to sweep out carriers generated by TPA.

Fig. 4 shows BER curves taken on the converted signal at 40 Gb/s for each of the four demultiplexer outputs D1–D4. The back-to-back curve is taken directly after modulation (no chip, filters, or amplifiers in the optical pathway) of a probe signal set to the same wavelength as the converted signal. A discrepancy is observed in the sensitivity of the receiver when monitoring the odd (D1, D3) and even (D2, D4) pins of the demultiplexer. Since the demultiplexer employs a half-rate clock (20 GHz), the 40-Gb/s data is sampled twice per clock period. One clock transition (rising or falling edge) is used to sample even bits, while the other is used to sample the odd bits. Therefore, the discrepancy between the odd and even pins is likely a result of nonunity mark : space ratio or uneven jitter between the rising and falling clock edges. Despite the discrepancy, the power penalty is similar for the two odd pins and for the two even pins (D1 and D3: 2.9 dB; D2: 4.0 dB; and D4: 4.7 dB).

#### IV. CONCLUSION

We have demonstrated the longest-spanning high-speed wavelength conversion reported to date in a dispersion-

engineered silicon photonic waveguide, and have quantitatively characterized the BER degradation resulting from the conversion. The primary cause of degradation is determined to be due to the limited conversion efficiencies, but improvements are expected in future active devices. These results provide a significant advancement toward the integration of ultrafast all-optical parametric processing devices within large-scale optical networking systems.

#### REFERENCES

- [1] C. Gunn, "CMOS photonics for high-speed interconnects," *IEEE Micro*, vol. 26, no. 2, pp. 58–66, Mar./Apr. 2006.
- [2] A. Shacham, K. Bergman, and L. P. Carloni, "Photonic networks-on-chip for future generations of chip multiprocessors," *IEEE Trans. Comput.*, vol. 57, no. 9, pp. 1246–1260, Sep. 2008.
- [3] A. C. Turner, C. Manolatu, B. S. Schmidt, M. Lipson, M. A. Foster, J. E. Sharping, and A. L. Gaeta, "Tailored anomalous group-velocity dispersion in silicon channel waveguides," *Opt. Express*, vol. 14, no. 10, pp. 4357–4362, May 15, 2006.
- [4] K. Yamada, H. Fukuda, T. Tsuchizawa, T. Watanabe, T. Shoji, and S. Itabashi, "All-optical efficient wavelength conversion using silicon photonic wire waveguide," *IEEE Photon. Technol. Lett.*, vol. 18, no. 9, pp. 1046–1048, May 1, 2006.
- [5] M. A. Foster, A. C. Turner, R. Salem, M. Lipson, and A. L. Gaeta, "Broad-band continuous-wave parametric wavelength conversion in silicon nanowaveguides," *Opt. Express*, vol. 15, no. 20, pp. 12949–12958, Oct. 1, 2007.
- [6] H. Rong, Y.-H. Kuo, A. Liu, M. Paniccia, and O. Cohen, "High efficiency wavelength conversion of 10 Gb/s data in silicon waveguides," *Opt. Express*, vol. 14, no. 3, pp. 1182–1188, Feb. 6, 2006.
- [7] Y.-H. Kuo, H. Rong, V. Sih, S. Xu, M. Paniccia, and O. Cohen, "Demonstration of wavelength conversion at 40 Gb/s data rate in silicon waveguides," *Opt. Express*, vol. 14, no. 24, pp. 11721–11726, Nov. 27, 2006.
- [8] M. A. Foster, A. C. Turner, J. E. Sharping, B. S. Schmidt, M. Lipson, and A. L. Gaeta, "Broad-band optical parametric gain on a silicon photonic chip," *Nature*, vol. 441, pp. 960–963, Jun. 22, 2006.
- [9] R. Salem, M. A. Foster, A. C. Turner, D. F. Geraghty, M. Lipson, and A. L. Gaeta, "Signal regeneration using low-power four-wave mixing on silicon chip," *Nature Photon.*, vol. 2, pp. 35–38, Jan. 2008.
- [10] M. J. O'Mahoney, C. Politi, D. Klionidis, R. Nejabati, and D. Simeonidou, "Future optical networks," *J. Lightw. Technol.*, vol. 24, no. 12, pp. 4684–4696, Dec. 2006.
- [11] B. G. Lee, A. Biberman, M. A. Foster, A. C. Turner, M. Lipson, A. L. Gaeta, and K. Bergman, "Bit-error-rate characterization of silicon four-wave-mixing wavelength converters at 10 and 40 Gb/s," in *Proc. Conf. Lasers Electro-Optics (CLEO 2008)*, San Jose, CA, May 2008, Paper CPDB4.
- [12] W. Mathlouthi, H. Rong, and M. Paniccia, "Characterization of wavelength conversion by four wave mixing in silicon waveguides," in *Proc. Conf. Lasers Electro-Optics (CLEO 2008)*, San Jose, CA, May 2008, Paper CThH3.
- [13] G. P. Agrawal, *Nonlinear Fiber Optics*, 3rd ed. San Diego, CA: Academic, 2001.